

Development and Characterization of Sugar Palm (*Arenga Pinnata* (*Wurmb. Merr*)) Fiber Reinforced Cassava (*Manihot esculenta*) Starch Biopolymer Composites

Saaed Abdullah Mousa^a, S. M. Sapuan^b, M. M. Harussani^{b,c}, Tarique Jamal^f, M. A. M. Azri^b, R. A. Ilyas^{d,e}, Muhammad Amin Azman^b, Vasi Uddin Siddiqui^b, and Tahrim Rafin^b

^aCollege of Engineering, Jazan University, Jazan, Saudi Arabia; ^bAdvanced Engineering Materials and Composites Research Centre (AEMC), Department of Mechanical and Manufacturing Engineering, Universiti Putra Malaysia, Serdang, Malaysia; ^cEnergy Science and Engineering, Department of Transdisciplinary Science and Engineering, Tokyo Institute of Technology, Meguro, Tokyo, Japan; ^dSchool of Chemical and Energy Engineering, Faculty of Engineering, Universiti Teknologi Malaysia (UTM), Johor Bahru, Malaysia; ^eCentre for Advanced Composite Materials (CACM), Universiti Teknologi Malaysia (UTM), Johor Bahru, Malaysia; ^fInstitute of Energy Infrastructure, College of Engineering, Universiti Tenaga Nasional, Kajang, Selangor, Malaysia

ABSTRACT

The study aims to develop a biopolymer composite made of sugar palm fiber and cassava starch that may degrade over time and to investigate the physical and structural characteristics of biocomposite films. Sugar palm fiber (SPF) was cast into a biocomposite with cassava starch (CS) as the matrix and fructose as the plasticizer using the casting process. The thermo-plastic CS composite sheet was loaded with different amounts of SPF (0%, 5%, 10%, 15%, and 20% dry starch). The addition of SPF considerably improved the physical and thermal properties. It enhanced the thickness of the material while lowering its density, water content, and biodegradability. However, there was no significant increase in the tensile properties of the composite films. The filler had been absorbed into the matrix, according to SEM micrographs. With a higher concentration of SPF, the SPF/CS films had a more heterogeneous surface. It is indeed possible that the addition of SPF changed the film characteristics of cassava starch, potentially compromising the performance of the films. Overall, the findings of this study concentrate on enlightening about biopolymer composite film and highlighting its great potential for the food packaging market.

摘要

该研究旨在开发一种由糖棕榈纤维和木薯淀粉制成的生物聚合物复合材料，该复合材料可能会随着时间的推移而降解，并研究生物复合膜的物理和结构特征。以木薯淀粉（CS）为基体，果糖为增塑剂，采用铸造工艺将糖棕榈纤维（SPF）铸造成生物复合材料。热塑性CS复合片材装载有不同量的SPF（0、5、10、15和20%干淀粉）。SPF的添加显著改善了物理和热性能。它提高了材料的厚度，同时降低了其密度、含水量和生物降解性。然而，复合膜的拉伸性能没有显著提高。根据SEM显微照片，填料已经被吸收到基质中。SPF浓度越高，SPF/CS薄膜的表面越不均匀。SPF的添加确实可能改变了木薯淀粉的薄膜特性，从而可能影响薄膜的性能。总之，本研究的结果集中于对生物聚合物复合膜的启发，并突出其在食品包装市场上的巨大潜力。

KEYWORDS

Sugar palm fiber; cassava starch; biopolymer; biocomposites; mechanical properties; food packaging

关键词

糖棕榈纤维; 木薯淀粉; 生物聚合物; 生物复合材料; 力学性能; 食品包装

CONTACT S. M. Sapuan  sapuan@upm.edu.my  Advanced Engineering Materials and Composites Research Centre (AEMC), Department of Mechanical and Manufacturing Engineering, Universiti Putra Malaysia, Serdang, Selangor 43400 UPM, Malaysia

© 2023 The Author(s). Published with license by Taylor & Francis Group, LLC.

This is an Open Access article distributed under the terms of the Creative Commons Attribution License (<http://creativecommons.org/licenses/by/4.0/>), which permits unrestricted use, distribution, and reproduction in any medium, provided the original work is properly cited. The terms on which this article has been published allow the posting of the Accepted Manuscript in a repository by the author(s) or with their consent.

Introduction

Biodegradable material is classified as composite since it is made up of resin and natural fibers. The depletion of petroleum supplies, combined with growing awareness of global environmental issues, prompted a quest for new green and environmentally friendly options (Harussani et al. 2022; Tarique et al. 2021). As a result, natural fibers have received much interest as reinforcing elements in polymers and composites (Nurazzi et al. 2021; Tarique et al. 2022c). Natural fibers are an attractive study topic because of their characteristics such as cheap cost, low density, easily available, sustainability, recyclability, as well as biodegradability, and significant efforts are being made to utilize their potential entirely (Harussani et al. 2021; Ilyas et al. 2020; Tarique et al. 2022a). However, the most challenging aspect of developing a biodegradable composite is the disparity in properties and characteristics of natural fiber reinforced polymer, since fiber is filled within the matrix. Various factors influence the properties of biocomposites, including the type of fiber used, how it is produced, fiber modification, and even environmental circumstances (Abotbina et al. 2022; Faruk et al. 2012; Hafila et al. 2022; Kamaruddin et al. 2022; Tarique et al. 2022a, 2022b). On the other hand, biocomposites are an excellent material for replacing commercialized petroleum-based materials in a variety of areas, including building, manufacturing, and even the automotive industry.

Sugar palm (*Arenga pinnata* (Wurmb. Merr)) trees are a local tree that has been around for hundreds of years. Generally, sugar palm fiber (SPF) and sugar palm starch (SPS) are two main products extracted from *Arenga pinnata* trees which recently has been focused by researchers as they show significant potentials in composite applications (Harussani et al. 2021; Sapuan and Bachtiar 2012). Sugar palm is abundant in countries such as Malaysia and Indonesia. Sugar palm fiber is depicted in Figure 1(a), was chosen as the reinforcement fiber because it possesses several desirable characteristics, including (i) excellent durability and resistance to seawater, (ii) high tensile strength, and (iii) good heat and moisture tolerance. Whereas cassava (*Manihot Esculenta*) is a versatile plant that can be used in various ways, as shown in Figure 1(b). In fact, it is the world's fifth-most-produced starch crop. One of the most promising environmentally friendly materials among natural polymers, starch has been recognized as such because of its affordability, availability, and biodegradability (Azlin et al. 2022; Panichnumsin et al. 2010; Tarique et al. 2021, 2022a). Cassava was chosen as the matrix primarily due to its high starch content (Veiga et al. 2016). However, the native starch films possess certain drawbacks, for instance brittleness and hydrophilicity. TPS film flexibility was enhanced by reducing internal hydrogen connections between polymer chains in order to increase free volume. The effect of plasticizers is due to their comparable structure to polymers (Jouki et al. 2013). Previous research found that starch is one of the most promising natural polymers due to its cheap cost,



Figure 1. (a) sugar palm fiber (*Ijuk*) and (b) cassava.

Table 1. Previous works on cassava starch-based biopolymer composites for food packaging applications.

Biopolymer	Natural fiber	Tensile Performance			Ref.
		Tensile strength (MPa)	Young's modulus (GPa)	Extension/Elongation at break (%)	
CS (90%)	SPF (5%)/CB (5%)	20	1.1	5	(Edhirej et al., 2017c)
CS (95%)	Cogon grass fiber (5%)	5	0.29	2.9	(Jumaidin et al., 2020)
TS (70%)	PALF (30%)	18.5	0.98	6.5	(Jaafar et al., 2018)
CS (97%)	KCF (1.54%)/Glycerol (1.47%)	3.80	2.86	1.53	(Walster et al., 2018)
TS (90%)	WHF (10%)	6.68	0.21	7.30	(Abraal et al., 2018)

*CS – cassava starch, TS – tapioca starch, SPF – sugar palm fiber, CB – cassava bagasse, PALF – pineapple leaf fiber, KCF – kenaf core fiber, WHF – water hyacinth fiber.

environmental friendliness, biodegradability, and ease of availability (Galdeano et al. 2009). However, starch-based films were shown to have a brittle structure, resulting in inferior mechanical characteristics. As a result, the use of plasticizers is required to overcome the brittleness problem in the films. The primary functions of plasticizers are to reduce intermolecular tensions and increase the mobility of polymer chains, which aids in lowering the glass transition temperature of plasticized starch films and so enhancing their flexibility (Sanyang et al. 2015; Tarique et al. 2021). Recent research has focused on the use of fructose as a plasticizer in biodegradable films (Gürler et al. 2023; Mohammed et al. 2023; Thakur et al. 2022). As a result of the increasing mobility of polymeric chains, the flexibility, ductility, and extensibility of plasticized films improved. Plasticizers added to starch-based films helped to minimize their inherent brittleness by increasing polymer-chain mobility, decreasing intermolecular pressures and glass transition temperature, and increasing flexibility.

SPF can be used to reinforce epoxy, but only with special treatment. Epoxy is hydrophobic, whereas the fiber is hydrophilic. The SPF reinforced unsaturated polyester with a 30% volume component is the specimen under investigation (Nagarjun, Kanchana, and Rajesh Kumar 2022; Rajeshkumar et al. 2021; Sahari et al. 2012). The tensile strength of sugar palm fiber reinforced unsaturated polyester (SPF/PE) is 11.473 MPa (Sahari et al. 2012). Sahari et al. (2012) also mentioned that the fibers added to the resin (polyester) lower the tensile strength than pure unsaturated polyester, which has the value of 24.835 MPa. This is most likely due to void contents in composites, which occurred after the evaporation of moisture during exothermic crystallization process of the unsaturated polyester. To place more emphasis, a summary of the previous works by numerous researchers on the cassava starch-based biopolymer composites has been presented in Table 1.

This research focuses on the utilization of biopolymer composites to develop film that decompose quickly in the environment and provide economic and environmental benefits to society. The primary goal of this study is to see how various sugar palm fiber loadings affect the composite's physical, mechanical, as well as structural properties. SPF and cassava starch are used to make the biopolymer composite utilized as materials for green food packaging. However, developing this biodegradable substance into films needs an understanding of how to treat these two elements appropriately so that they can be combined properly.

Materials and methods

Materials

SPF was collected at Jempol, Negeri Sembilan, Malaysia and utilized as reinforcing fibers in films. The fibers were dried and then the fibers were grinded to fine particles. SPF was ground into a powder with particle sizes between 150 μm and 300 μm using a 50/100 mesh screen to measure the particle size. As

Table 2. Chemical composition of cassava starch (Chinma, Chukwuma Ariahu, and Oneh Abu 2013; Edhirej et al. 2017a).

Constituents	Composition (%)
Amylose	29.5
Carbohydrate	9.8
Moisture	7.1
Protein	0.32
Crude fiber	1.2
Lipid	0.17
Ash	0.45

detailed in a previous study (Edhirej et al. 2017c, 2017b), cassava starch was produced from local cassava tubers. According to the previous research of Edhirej et al. (2017) and Chinma, Chukwuma Ariahu, and Oneh Abu (2013), the chemical compositions of cassava starch are as follows (Table 2):

Films preparation

The films were prepared using cassava starch that can easily be bought at a convenient local store. The plasticizer chosen for this composite film was fructose at concentration of 0.30 gg^{-1} dry starch. It is said that the amount of plasticizer needed is around 10–60% on a dry basis, depending on stiffness of polymers. In comparison to other plasticizers, films made with fructose have better mechanical and thermal durability, produce smooth, uniform surfaces free of holes, and absorb less water (Ibrahim et al. 2019a).

The casting method was utilized to develop these composites film as it is fast and straightforward. The film preparation processes are as follows: (i) 5 g of cassava starch/100 ml distilled water was heated to 80°C and stirred continuously in a water bath for 20 min, (ii) film-forming solution is placed into a desiccator under a vacuum in case any air bubble are formed during the heating until no more bubbles were present, (iii) the solution was poured onto a plate which was later dried in an oven at 50°C with air circulation for 24 h, (iv) films were peeled out from plate and put at ambient condition (25°C as well as relative humidity of 60%) for a week in a plastic bag, and (v) the casting technique was repeated but this time adding 5%, 10%, 15% and 20% of powdered sugar palm fiber into the solution as indicated in Table 3.

Films characterization

Films density

The film sample size of (20 mm × 20 mm) was used to determine the film density based on Equation (1):

$$\rho = \frac{m}{V} \quad (1)$$

where m and v are the film sample's weight (g) and volume (cm^3), respectively. The volume of the sample was calculated by dividing the film area by the thickness of the film.

Table 3. Cassava starch-based film samples.

Biopolymer films	Fructose (g)	Cassava starch (g)	Sugar palm fiber (%)
CS	1.5	5.0	0
SPF-5/CS	1.5	5.0	5
SPF-10/CS	1.5	5.0	10
SPF-15/CS	1.5	5.0	15
SPF-20/CS	1.5	5.0	20

Film thickness

A digital micrometer (Mitutoyo Co., Japan) was used to measure thickness of film samples with an accuracy of 0.001 mm. Five replicate measurements were made for each film sample, as well as a mean value was computed. As thickness is same across all the films, there was no required of the particle distribution test (Roslim et al. 2018).

Moisture content

Film moisture content (MC) was determined using the weight loss of the film. Initially, the samples were weighed (W_i). It is then dried at 105°C for 24 h and weighed again (W_f). Thus, the moisture content can be determined by amount of water loss between (W_i) and (W_f) using Equation 2.

$$MC(\%) = \left[\frac{(W_i - W_f)}{W_i} \right] \times 100 \quad (2)$$

Fourier transform infrared spectroscopy

A spectrometer (Thermo Fisher Scientific, model Nicolet 6700, Rockford, IL, USA) was used to record the FTIR spectra of the specimens to investigate the functional groups in the biopolymer composite specimens. With a spectral resolution of 4 cm^{-1} , each specimen was scanned 16 times between 4000 and 650 cm^{-1} .

Scanning electron microscopy

At 15 kV of an acceleration voltage, the scanning electron microscope, SEM (Hitachi), was used to examine the morphology of the films. The film samples were mounted to the aluminum stubs using double-sided adhesive tapes. In order to stop charging, samples were then covered with a thin coating of gold (0.01–0.1 μm).

Tga

TA Instruments (Mettler-Toledo AG, Schwerzenbach, Switzerland) were used in the thermogravimetric analysis method to determine the thermal stability of the film samples. The test parameters were recorded while the temperature was changed in a nitrogen gas medium from 25°C to 600°C at a constant heating rate of 10°C/min. A 10 mg sample of the film was heated in an aluminum tray. TGA study shows the weight loss in relation to temperature.

Soil burial test

The films with an identical volume and known weight (W_i) are buried 100 mm under the surface of the soil for 1, 2, 3, and 5 days where water is added at 0, 200, 400, 600, 800 and 1000 h. The buried samples were watered every 2 days. The films are wiped gently and dried to a constant weight at 60°C in a vacuum oven after it has been taken out accordingly and reweighed (W_f). Weight loss was determined utilizing Equation 3.

$$\text{Weight loss}(\%) = \left[\frac{(W_f - W_i)}{W_i} \right] \times 100 \quad (3)$$

Tensile test

The mechanical properties of the films were determined using a tensile machine. The films are to be cut into 50 mm \times 12.7 mm and tested on a 5 kN INSTRON tensile machine with an initial grip separation and crosshead speeds of 30 mm and 500 mm min^{-1} . The test was done at least five times to get the average value.

Statistical analysis

SPSS software was used to do an analysis of variance (ANOVA) on the experimentally collected data. Duncan's test was used to compare means at a 5% level of significance ($p \leq .05$).

Results and discussions

Physical properties of biocomposite films

Film thickness and density

Table 4 shows that when fiber was added, films thickness grew while density decreased as well as showed modest fluctuations. The thicker the cassava starch biopolymer film, the higher the fiber contents. With a thickness of 0.151 mm and no fiber loading, the CS film was the thinnest. However, with a thickness of 0.202 mm, the film with 20% SPF loading (SPF-20/CS) was the thickest. The use of a large amount of filler resulted in thicker biopolymers. According to Versino and Alejandra García (2014), speculate that structural flaws may result from the presence of large filler particles in the polymer matrix.

Density is the measure of the relative "heaviness" of objects having the same constant volume. Density can also be defined as how crowded a material appears to be. In addition, the CS film had highest density of 1.528 g/cm^3 , while the films with 20% SPF loading (SPF-20/CS) had the lowest density of 1.280 g/cm^3 , as shown in Table 4. The densities of film and the percentage of fiber loading are inversely proportional. The density decreases as the fiber loading increases. This is due to the sugar palm fiber's physical properties in terms of its density (Mohd Nurazzi et al. 2018). Since sugar palm fiber has pores inside it, increasing fiber loadings in the film are to surely decrease the density of the films. To place more emphasis, Edhirej et al. (2017c) mentioned that when the filler proportion increased, density of composites reduced due to the lighter density of the filler material. In comparison to the CS film, the density of the hybrid composite film dropped (31.79%) as the fiber content increased (Edhirej et al. 2017c). Similarity can be found between the CS/SPF and CS-CB/SPF film composites regarding the density and thickness of composites film. Density of composites dropped as filler content increased; this could be owing to filler material's lower density (1.26 g/cm^3 for SPF) (Ishak et al. 2012; Sahari et al. 2012). Film with a higher fibers content had lower density. In other words, when compared to pristine CS film, density of composites films reduced as the fiber concentration increased. Shakuntala, Raghavendra, and Samir Kumar (2014) reported similar results for wood apple shell reinforced epoxy composite, and by Salgado et al. (2008), found comparable results for foams made of cassava starch, sunflower proteins, and cellulose fibers.

Moisture Content (MC)

Table 4 shows weight values of samples before and after it was dried in an oven at 105°C for 24 h. Equation 2 is used to calculate moisture content. When selecting natural fibers as a reinforcing material, the moisture content of the fiber is a significant factor to consider. This is because the moisture content of natural fibers in a composites materials impacts its dimensional stability, tensile strength, swelling and electrical resistivity (Jawaid and Abdul Khalil 2011). The MC of SPF loading films was lower compared to neat CS film, with 22.65–31.58%, respectively, according to moisture content of fibers.

Table 4. Physical characteristics of CS film, and SPF/CS composites film.

No.	Films	Thickness (mm)	Mass (g)	Density (g/cm^3)	Moisture Content (%)
1	CS	0.151 ± 0.008^a	0.146 ± 0.012^a	1.528 ± 0.175^a	16.908 ± 5.441^a
2	SPF-5/CS	0.152 ± 0.006^a	0.147 ± 0.016^a	1.522 ± 0.112^a	13.078 ± 5.717^a
3	SPF-10/CS	0.174 ± 0.014^b	0.150 ± 0.012^a	1.354 ± 0.036^a	13.620 ± 6.560^a
4	SPF-15/CS	0.186 ± 0.013^b	0.159 ± 0.013^a	1.349 ± 0.076^a	19.302 ± 5.971^a
5	SPF-20/CS	0.202 ± 0.013^c	0.164 ± 0.009^a	1.280 ± 0.050^a	11.468 ± 7.310^a

Based on Table 4, moisture content of samples is highest with 15% of fiber loading. The moisture for neat CS film with 0% fiber loading is higher than the other samples except for 15% loading. When fiber concentrations increased from 5% to 20%, moisture content of the sugar palm cassava film slightly increased, as shown in Table 4. The reason SPF-15/CS has the highest moisture content is because all-natural fiber is made up of hydrophilic natural polymeric materials such as celluloses, hemicelluloses, and lignin. All of these substances are vital in the absorption of water. Because these elements have a lot of –OH groups, they may easily attach water molecules (Roslim et al. 2018). Thus, the ability to absorb moisture increases. However, the film of 20% has the lowest moisture content of all. This is probably owing to inconsistency of the sizes of the SPF powder. A larger fiber size means more fiber agglomeration, which in turn lowers the moisture content of film. The powder used was apparently mixed with dust and large sizes of sugar palm fiber. This was probably due to mishandling and human error during the production of fibers from the raw fiber into powdered form.

The moisture content of the CS films dropped slightly when SPF fillers were added, as indicated in Table 4. In comparison to the CS film and the films with lower SPF content, the film with a greater SPF content had a lower MC. The matrix successfully stopped water molecules from diffusing into cell wall as well as cell lumen, or at the very least, decreased permeability of fibers after micro-pores were plugged. Moisture content of films containing SPFs was substantially lower than those of the neat CS film after bulking hydroxyl group of the cell wall. This conclusion is consistent with that of Soykeabkaew, Supaphol, and Rujiravanit (2004), who reported that the MC of tapioca starch-based foam reinforced with flax and jute decreased with time and with Kaisangsri, Kerdchoechuen, and Laohakunjit (2012) investigated moisture content of cassava starch, natural fiber, and chitosan-based biodegradable foam trays. Despite having highest equilibrium moisture level, films with lowest fiber addition were more soluble compared to those with the highest fiber addition. These findings are similar to those reported by Edhirej et al. (2017a) for cassava bagasse/SPF reinforced cassava starch hybrid composites.

Generally, starch-based films have an excellent property to be soluble in water. In order for this particular composite to function appropriately as a packaging material, water insolubility may be required for a potential application. When the films are exposed to water, they are found to be unable to maintain their integrity. With an increased concentration of fiber, the solubility decreases. Thus, by right, films with higher concentrations should be less prone to have high solubility in water.

Ftir

Composite is the combination of substances, usually two or even more. FTIR is done in order to know whether the sample produced has a certain functional group. By knowing the functional group, we can identify the possible interactions between the fiber and matrix. FTIR was used to examine the functional groups in the SPF/CS composites (Figure 2). The presence of specific chemical components in the biocomposites, including amylose and amylopectin for starch and cellulose, hemicellulose, and lignin for the fiber, was demonstrated in this section.

The strong peak at 3355.47 cm^{-1} is related to the stretching of the O-H groups in starch and fiber. This shows that starches are very sensitive to water molecules because they have hydroxyl groups. This was supported by previous studies (Jaiswal et al. 2022; Syafri et al. 2018). The stretching of hydroxyl groups owing to hydrogen bonding between molecules was attributed to these peak ranges. Meanwhile, the C-H stretching was attributed to the strong bands at $2900\text{--}3000\text{ cm}^{-1}$, and the peaks at $990\text{--}1000\text{ cm}^{-1}$ were determined to be typical of a hydro-glucose ring O – C stretch (Tarique et al. 2022). From the spectra in Figure 2(a), the stretching of C – H groups is seen at 2939.07 cm^{-1} . The C-H bonding can also be seen at 1368.48 cm^{-1} and the final peak being focused on is 1078.97 cm^{-1} . This is attributed to the C – O bond stretching of the C – O – H group in cassava starch. The peaks at 1542 cm^{-1} were also attributed to water bending in starch (Ayu et al. 2020). Furthermore, this band is wider in the CS film than in the composite samples due to the structure of the polysaccharide and the potential for water interaction with this poly-hydroxylated system. The

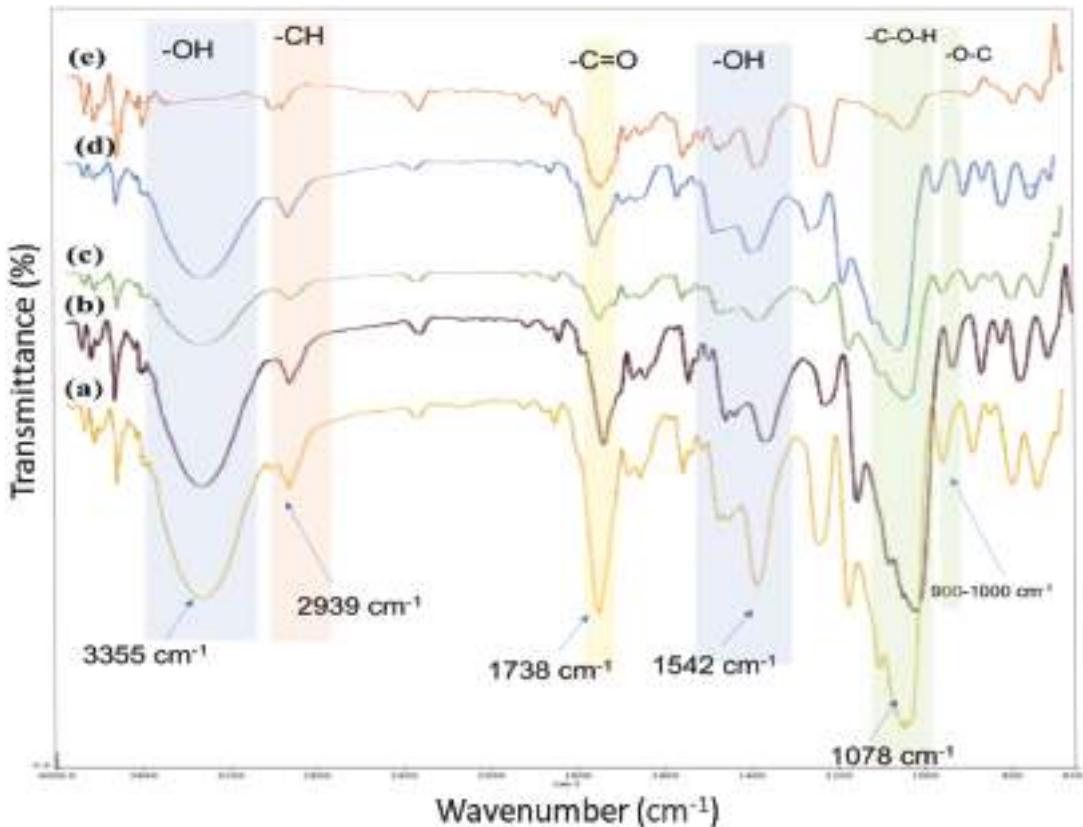


Figure 2. FTIR of biopolymer film samples; (a) CS, (b) SPF-5/CS, (c) SPF-10/CS, (d) SPF-15/CS, and (e) SPF-20/CS.

increase in fiber content in composites has an inverse relationship with the shape of this band. Tongdeesoontorn et al. (2012) mentioned that the adsorbed water in the samples is represented by the band at 1642 cm^{-1} . The CS film, as shown in the spectra, has the strongest peak at this frequency, as seen by the breadth and intensity of the O–H band at 3359 cm^{-1} . The SPF/CS composite, on the other hand, shows a reduction in this range. Furthermore, the strength of the band varies gradually (decreasing) as the number of fibers increases in these CS films. This data implies that the starch is primarily responsible for this water band and that the SPFs, because of their low moisture content, have no discernible influence.

If we compare all the FTIR spectra of the films with the control film (0%), the differences that can be seen are the width and position of the band around 3355.47 cm^{-1} , 1739.50 cm^{-1} and 1368.48 cm^{-1} . The O–H stretch is linked to 3355.47 cm^{-1} , which is the free hydroxyl. The intense peaks around $3400\text{--}3500\text{ cm}^{-1}$ show the presence of O–H groups in the starch. In other words, it also indicates that starches are highly hydrophilic.

Morphological properties

The microstructure and interfacial adhesion of cassava starch and its reinforced biocomposites were studied using SEM. The samples were prepped into a size of $50\text{ mm} \times 12.7\text{ mm}$ for each film. The resulted observation images of sugar palm fiber cassava under the microscope have shown that the fiber does indeed disperse throughout the samples, but due to mishandling of materials, particularly the powdered form of sugar palm fiber, some parts of the samples are not fully supported by the fiber as it does not fully embed in the films. SEM micrographs of plasticized cassava starch (CS) films are

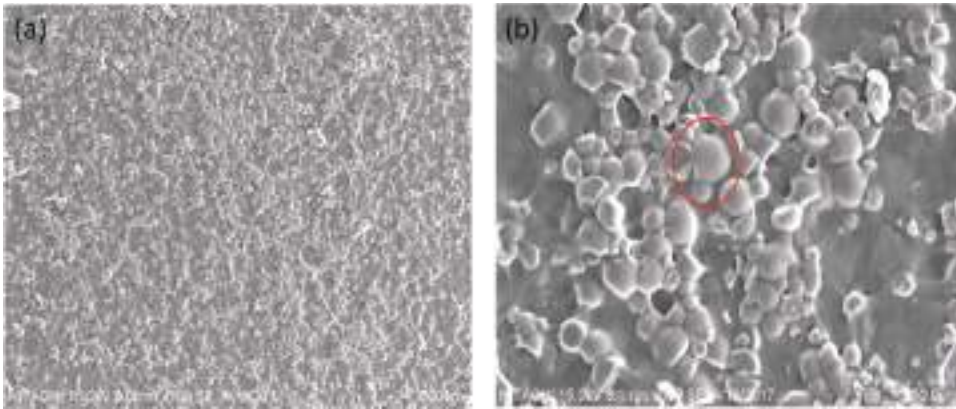


Figure 3. SEM images of CS for magnification of (a) 100 \times , and (b) 600 \times .

shown in [Figure 3\(a\)](#). The CS film has a compact structure and uniform surfaces. To be noted, the sample shows a bubble-like structure in it. This is due to overheating the mixture during the casting process. Although the sample's preparation was done according to the proper methods, different materials have different boiling points.

As a result of the filler addition, more heterogeneous surfaces were created, as shown in [Figures 4–5](#), where particles of reinforcing materials covered by starch matrix can be seen. The fibers were incorporated into starch matrix due to the extraordinary compatibility of both components, indicating that the fibers seemed to agglomerate with starch. A resistant interface is achieved by good adhesion between filler and matrix ([Kuciel and Liber-Knec 2009](#)). As a result, strengthening the matrix improves the material's mechanical characteristics. When a greater concentration of SPF filler (SPF-20/CS) was applied, particle density increased, encouraging filler particle interaction and the formation of aggregates. Because of their enormous volume, the existence of these aggregates, in combination with big fiber particle, causes flaws in the matrix, which compromise film structural integrity, as illustrated in [Figure 5](#). [Ludueña, Vázquez, and Alvarez \(2012\)](#) pointed out that the agglomerates prevent proper matrix–filler interaction, resulting in poorer polymer–filler interfacial adhesion.

[Figure 3\(a,b\)](#) shows the SEM image of SPF-5/CS biopolymers. The surface of the film was uneven. The uneven structures demonstrated that AS matrices had a poor interfacial adhesion. While in case of SPF-10/CS sample, fiber can be seen having two different sizes on the film ([Figure 4\(a\)](#)). This is still due to the usage of inconsistent fiber size during casting. Although some parts are embedded with the fiber, it can still cause fluctuation in strength of the film.

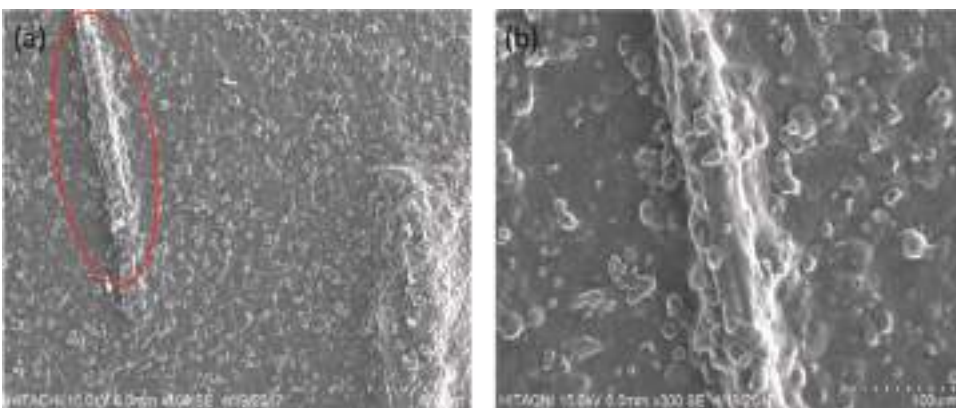


Figure 4. SEM images of SPF-5/CS for magnification of (a) 100 \times and (b) 300 \times .

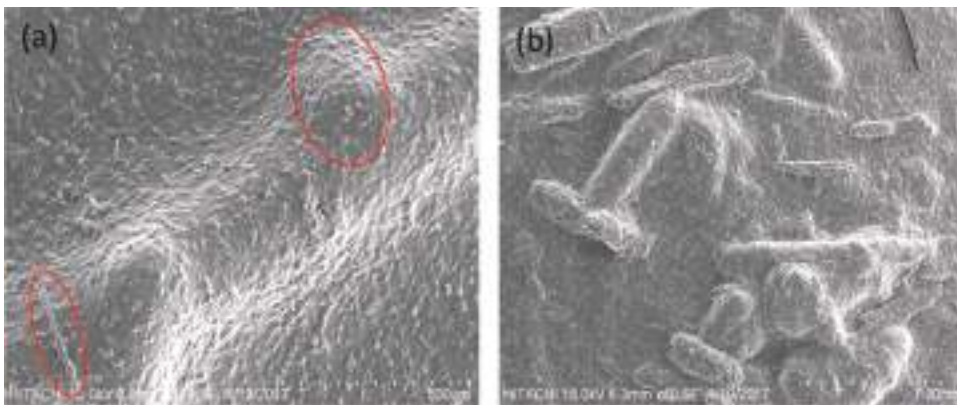


Figure 5. SEM image of (a) SPF-10/CS at magnification of 100x, (b) SPF-20/CS at magnification of 40 × .

As for SPF-20/CS film, the fibers are clustered together, which are mainly caused by the high fiber loading, as shown in [Figure 4\(b\)](#). Too much fiber in a structure can cause structural defects, which leads to loss of strength. As the aforementioned discussion, SPF-20/CS film sample was supposed to have the highest tensile modulus, but due to different sizing of fiber, the structure fails to show the expected result.

Tga

The thermal stability degradation temperatures of CS and SPF/CS biopolymer composite films at different fiber loadings are shown in [Figure 6](#). The TGA curve originated by charting the weight loss (mg) of composite film specimens versus temperature ($^{\circ}\text{C}$), while the DTG curve was formed by charting the derivative of weight loss (mg) as a temperature-dependent ($^{\circ}\text{C}$). Due to the removal of water molecules from the biocomposite film samples, the first degradation process took place at temperatures below 100°C . Additionally, weight loss at this stage may be related to biocomposites' loosely bound water and low molecular weight compounds vaporizing or being dehydrated. This also occurred with the CS film and all other film samples. Additionally, it can be seen that biocomposite films began to decompose between 32.94°C and 35.76°C , which was higher than the CS control film, which started to decompose at 31.38°C . This showed that the matrix and fibers were interacting well. A large peak was seen in the DTG curve of the CS film after further heating, which corresponded to a weight drop of about 78% and was most likely caused by saccharide ring breakdown in the CS biopolymer film. In comparison to SPF/CS biocomposite films, the CS biopolymer loses greater mass at temperatures below 100°C . These patterns of behavior could be related because CS biopolymer contains more moisture than biocomposite specimens (Hazrati et al. 2021 Ilyas et al. 2018).

The second thermal deterioration of the specimens occurred between 180°C and 260°C and was associated with the volatilization of fructose as well as chemisorbed water molecules. This temperature range for fructose breakdown of CS and SPF/CS biocomposite films confirmed the results of Podshivalov et al. (2017) on potato and Ilyas et al. (2018) on sugar palm starch, respectively. Similarly, Zhong and Yunfei (2014) reported that the thermal degradation of kudzu starch-based biopolymers plasticized with glycerol occurred between 150°C and 280°C . The large weight losses of both CS biopolymer and SPF/CS biocomposites indicate that the greatest thermal disintegration rate was achieved at temperatures over 280°C .

According to [Figure 6a](#), the start of the thermal degradation of CS biopolymers occurred at about 300°C . This might be due to the loss of hydroxyl groups, depolymerization, and disintegration of the polymeric carbon chain of starch, the major ingredient of biocomposites (Prachayawarakorn et al. 2013). The optimal breakdown temperatures for CS and SPF-20/CS were 317°C and 318°C ,

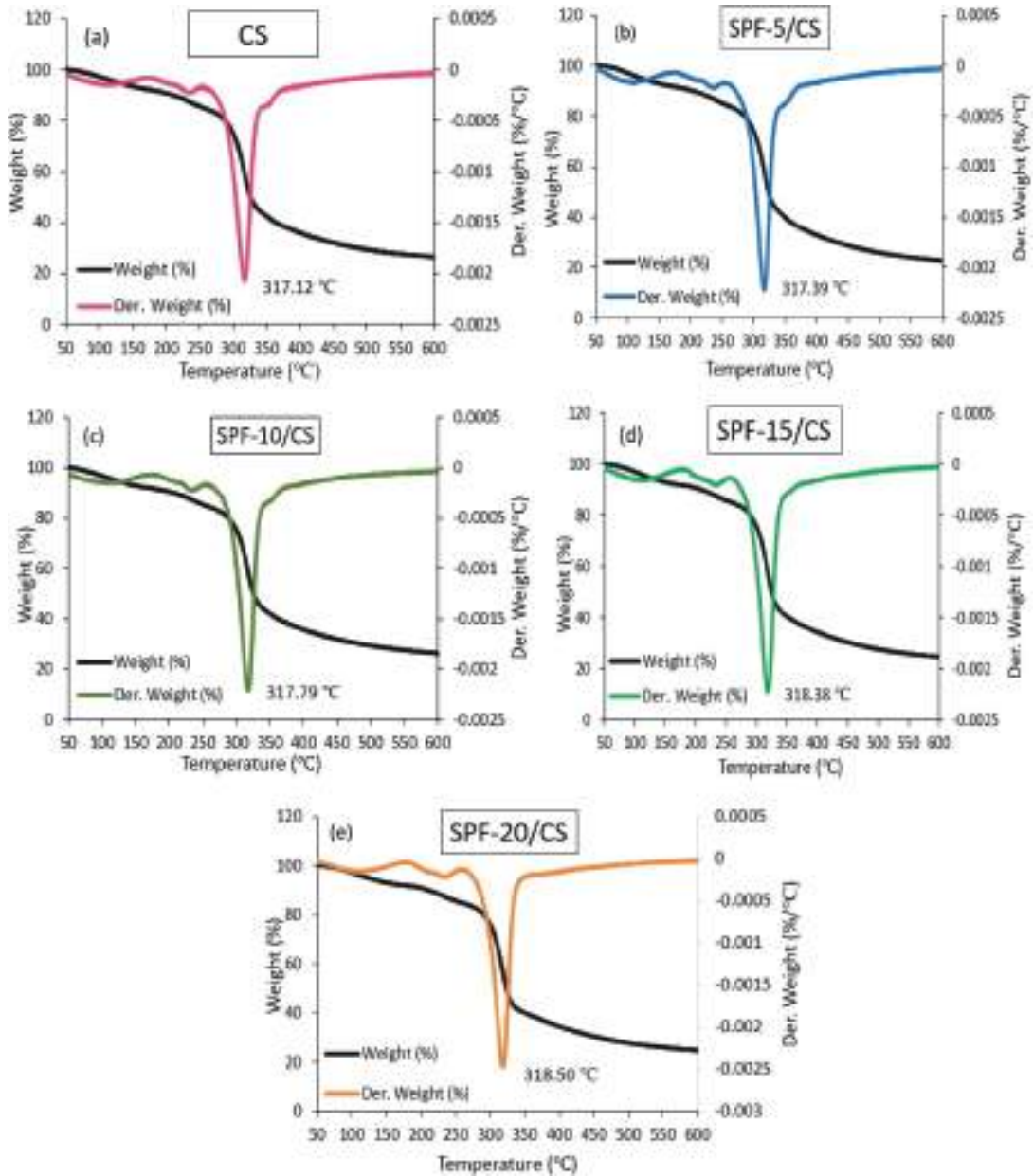


Figure 6. TGA and DTG curves of biocomposite films containing CS and SPF/CS with various fiber loadings.

respectively, demonstrating that the SPF-20/CS biocomposite film was more thermally stable than the CS biopolymer film. Meanwhile, the DTG peak of the SPF-20/CS bio-composite got to a higher temperature, demonstrating greater thermal stability than other film formulations. This may be attributed to the matrix's and fibers' strong adherence. The thermal stability of biocomposite films was also shown to improve as fiber loadings increased. Previous research also discovered that strengthening husk fiber into corn starch-based film and cellulose nanofibril into chitosan/oregano essential oil improved the thermal stability of film samples (Chen et al. 2020; Ibrahim et al. 2019b). Nonetheless, Table 5 shows that increasing the percentage of SPF reduced the weight loss of biocomposites at temperatures over 300°C, resulting in an improvement in the thermal stability of

Table 5. Weight loss (WL), mass residue, and temperature on maximum degradation (T_{Max}) for CS and SPF/CS biocomposite films were determined using TGA and DTG curves.

Sample	Water evaporation			First thermal degradation			Second thermal degradation			DTG Peak temperature	Mass residue
	T _{Onset} (°C)	T _{Max} (°C)	W _L (%)	T _{Onset} (°C)	T _{Max} (°C)	W _L (%)	T _{Onset} (°C)	T _{Max} (°C)	W _L (%)	(°C)	(%)
CS	31.38	107.85	8.5	178.73	232.24	6.9	258.73	317.12	59.7	317.12	22.47
SPF-5/CS	32.94	108.87	8.7	177.40	234.71	6.5	256.99	317.39	60.7	317.39	24.54
SPF-10/CS	34.52	103.21	8.8	175.89	233.82	6.6	254.54	317.79	58.8	317.79	26.11
SPF-15/CS	35.93	105.28	8.7	173.69	235.23	7.1	255.58	318.38	62.2	318.38	25.00
SPF-20/CS	35.76	110.53	8.2	177.11	237.10	6.5	251.33	318.50	59.1	318.50	26.57

biocomposites. Char is the substance that remains after pyrolyzing all volatile chemicals in the material (Harussani et al. 2021). The quantity of char residue in SPF/CS biocomposites increased with the incorporation of SPF, rising from 22.47% to 24.54% when 5% SPF was added to CS. The improved thermal strength of SPF/CS biocomposite films might be related to the presence of large carbonates in the SPF, which complemented to the thermal decomposition findings of the biocomposite. These results supported prior study that found that integrating natural fibers into the matrix increased the thermal stability of the biopolymer matrix (Dularia et al. 2019; Han and Bin Song 2021). It can be summarized that adding SPF to biocomposite films improved their thermal characteristics, which is an essential feature of food packaging materials. It may also allow high temperatures during the manufacturing of composites.

Tensile properties

Samples were prepared into a size of 50 mm × 12.7 mm, and a tensile test was conducted using initial grip separation and crosshead speeds of 30 mm and 500 mm min⁻¹. Based on the data from Figures 7–9, the average value for tensile stress, strain and Young's Modulus was calculated.

The tensile characteristics of SPF/CS biocomposites, such as tensile strength, tensile modulus, and film extension, are shown in Figures 7–9. In general, it can be shown that changes in the composition of SPF loading resulted in changes in the material's tensile characteristics. With an increase in SPF fiber content from 0% to 5%, composite tensile strength insignificant ($p < 0.05$) increased from 11.33 to 11.78 MPa, but film elongation at break decreases from 12.38 mm to just 3.50 mm significantly ($p < 0.05$). Figure 7 shows the average value of tensile stress for each respective film. The increase in tensile strength indicates that the bonding between the starch matrix and sugar palm fiber is strong enough, which enables the transfer of strength from the cellulose fiber to starch (Mohd Nurazzi et al. 2018). However, Figure 7 shows that the strength decreases steadily for 10–20% fiber loading. This could be related to the number of particles present in the film, which causes the films to be less homogenous material. Higher content of particles can also lead to structural defects. This claim is on par with the result from Edhirej et al. (2017a) for his study regarding cassava starch films.

Tensile modulus was also increased significantly ($p < 0.05$) from 255.84 to 397.27 MPa with the addition of SPF fiber. Figure 8 demonstrates that the Young's modulus rises from the control film to 15% fiber loading. The graph then drops a little from 15% to 20%. According to Sahari et al. (2014), the capability of a material to resist deformation in terms of tension is what tensile modulus is all about. They also said that the stiffer the material is, the higher the value of its tensile modulus. The highest tensile modulus amongst the films is the 15% fiber loading having the value of 427.22 MPa. By right, the more fiber is infused with the resin matrix, the higher the tensile modulus would be. But, in this case, the tensile modulus of the 20% fiber loading has a lower value than 15%. This is due to the inconsistencies of fiber size used during the casting process. With respect to extension of films at the break, the addition of fiber into the films does not help to make it more ductile. The control film (0%) stretches the most out of all samples. Figure 9 shows that with the increase of fiber loading, the

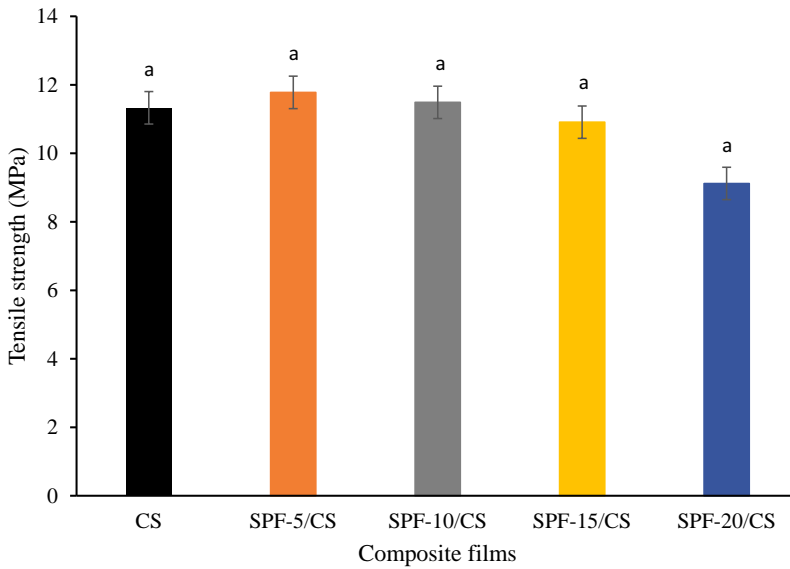


Figure 7. Average tensile strength of biopolymer composite films. Values with different letters in the figures are significantly different ($p < .05$).

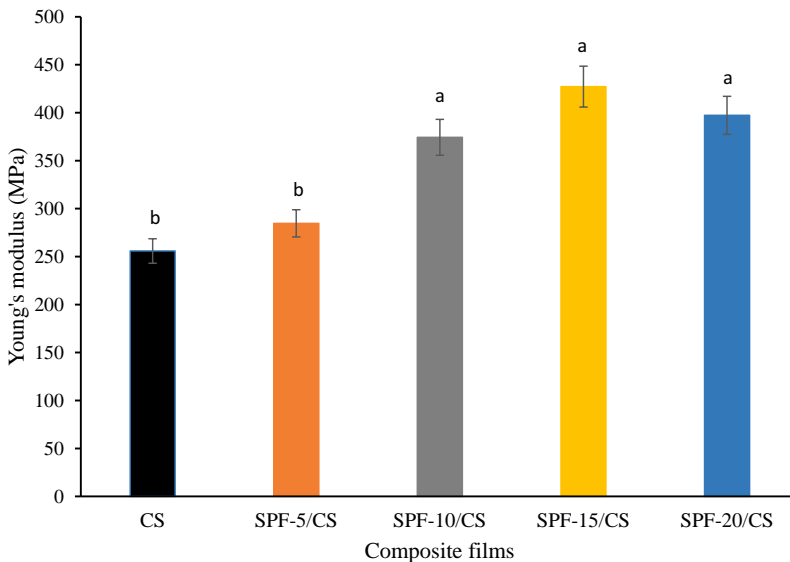


Figure 8. Young's modulus of biopolymer films. Values with different letters in the figures are significantly different ($p < .05$).

elongation at break decreases linearly until 20% fiber loading. We can say that with the addition of sugar palm fiber, the ductility decreases for the films.

Comparing the results of tensile strength and young modulus with the work shown in [Table 1](#) gives quite a lot of explanation and similarities. The average tensile strength shown in [Figure 7](#) is around 9–12 MPa whereas, in [Table 1](#), the CS (90%)-SPF (5%) &CB (5%) biocomposite has tensile strength of around 20 MPa reported work by Edhirej et al. (2017c). The reason this biocomposite has higher strength is because 5% CB is added which makes the bond stronger. Compared with another biocomposite CS (95%)-Cogon Grass fiber (5%) work done by Jumaidin et al. (2019) which tensile strength is 5 MPa. The

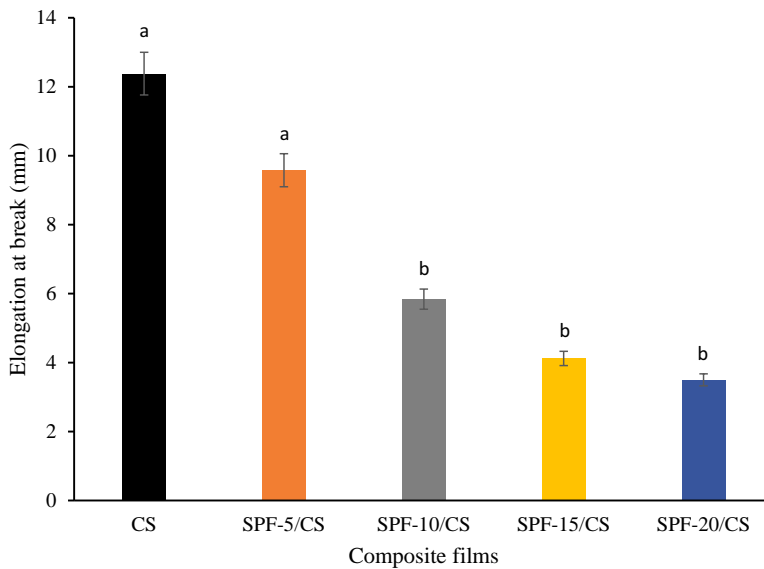


Figure 9. Maximum elongation at break of biopolymer films. Values with different letters in the figures are significantly different ($p < .05$).

tensile strength is lower compared to the average result shown in Figure 7. This is because the SPF structural fiber is more compatible than Cogon grass fiber with Cassava starch. Coming to Young's modulus which shows similar characteristics like the tensile strength properties. The CS (90%)-SPF (5%) & CB (5%) bio-composite Young's modulus was reported 1.1 GPa or 1100 MPa whereas the average Young's modulus of the CS/SPF biocomposite is around 250 to 425 MPa from Figure 8. As it can be seen there is a huge difference in Young's modulus and this is likely due to the addition of CB. In the case of the CS (95%)-Cogon Grass fiber (5%) Young's modulus, which was reported 0.29 GPa or 290 MPa is almost similar to the results shown in Figure 9.

Several factors may have contributed to the composites' increased tensile strength and modulus. To begin, the fiber and the thermoplastic CS matrix create a strong bond, resulting in efficient matrix-fiber stress transmission. The presence of fiber fracture in the SEM picture of the tensile fracture surface proved this. Second, the presence of fiber breakage indicates that the fiber and matrix are compatible. This might be because the CS matrix and the SPF fiber have comparable hydrophilic properties. Furthermore, the decreases in tensile strength and modulus might be attributed to the chemical structure of natural fiber and starch being comparable (Sapuan and Bachtiar 2012). This is owing to the fact that both natural fiber and starch have the same primary cellulose structure, which is made up of hydroxyl functional groups (Norizan et al. 2021). Meanwhile, the reduction in extension with the addition of CGF fiber might be due to fiber-matrix bonding, which prevents the material from elongating fully. As a result, the composite lost ductility compared to the CS matrix. The tensile results were consistent with a recent work by Prachayawarakorn and Pattanasin (2016), which found that adding cotton fiber to thermoplastic rice starch improved the tensile modulus and reduced elongation.

Biodegradability properties

The key indication for the biodegradation process by moisture and microorganism throughout the soil burial phase is material weight loss (Bootklad and Kaewtatip 2013; Maran et al. 2014). Each sample was buried 10 cm underneath the soil and was later taken out at the interval of 1, 2, 3 and 5 days, represented in

Table 6. Biodegradability test of the composite films.

No	Films	Weight loss (%)			
		Day 1	Day 2	Day 3	Day 5
1	CS	28.99	36.31	42.11	46.00
2	SPF-5/CS	30.48	39.35	42.77	54.27
3	SPF-10/CS	27.21	32.43	42.03	53.33
4	SPF-15/CS	27.22	35.48	65.81	74.38
5	SPF-20/CS	28.19	34.21	36.78	71.11

Table 6. After five days of soil burial, weight loss of SPF-reinforced CS biopolymer composites is shown in **Figure 10**. After five days of burial testing, all composites showed increased weight loss. It has been revealed that as the amount of fiber increases, also increases the percentage of water absorption. The inclusion of a hydroxyl group in the SPF causes this. The number of hydroxyl group increases as fiber loading increases, resulting in an increase in water absorption. More the water absorption more the microorganisms react with the composite to degrade which results in faster weight loss. The moisture present in the soil subsequently decimates the polyester chain, resulting in microscopic composite fragments. Through deterioration, soil microorganisms may consume them as a source of energy (Haque et al. 2021). This result can be attributed to a greater number of microorganisms active at a longer burial duration, resulting in an increase in material weight loss.

In general, adding SPF to a CS matrix has resulted in increased weight loss in composites, implying a more aggressive biodegradation process in the material. Weight reduction was increased by 46–70% when SPF fiber was included at a percentage of 0–20%. This conclusion might be related to SPF’s more hydrophilic behavior than the thermoplastic CS matrix, which enhances the hygroscopic properties of the composites, stimulates the development of microbes during degradation, and increases material weight loss (Maran et al. 2014). This finding implies that the SPF is very effective at speeding up the biodegradation of biocomposites. A similar finding was reported in previous studies for incorporation of agar (Maran

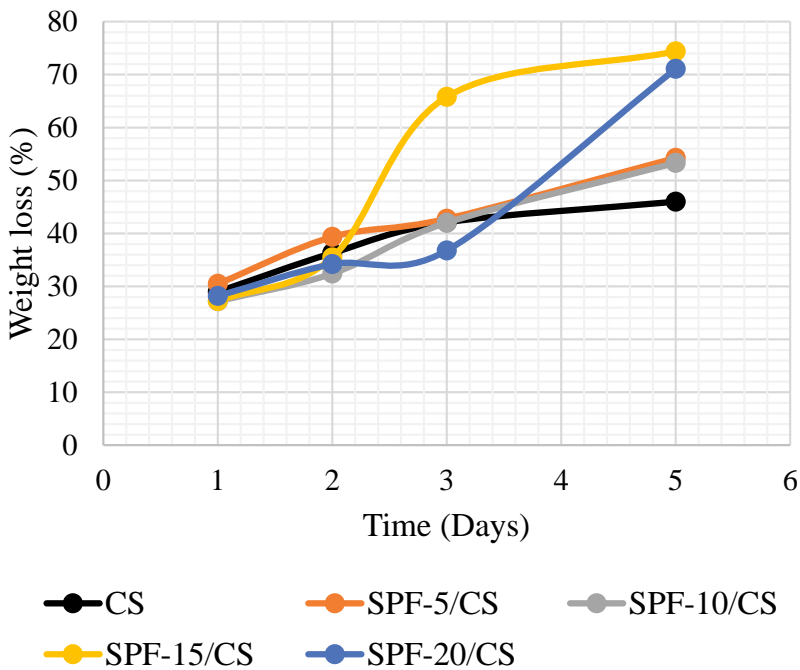


Figure 10. Weight loss of biopolymer films.

et al. 2014), fly ash (Sundum, Mészáros Szécsényi, and Kaewtatip 2018), char (Harussani et al. 2021) and coir fiber (de Farias et al. 2017) incorporated with a thermoplastic starch matrix.

If we study the line, from the 1st day until the 2nd day, the rate of degradation is almost the same for every sample but, when the phase reaches the 3rd and 5th day, the degradation of films increases drastically, especially for SPF-15/CS and SPF-20/CS samples. Films with higher fiber loading degraded faster with lost about three-quarters of their original weight. The films are broken down by microorganisms with water as the medium. Another reason for such increment for SPF-15/CS on the 3rd day maybe there is some unwanted parameters occurred during soil burial test most likely human error. With that in mind, these composite films made from sugar palm fiber cassava favor the environment. Thus, successfully reaching the objective of this study which was to produce a biodegradable composite that can degrade over time.

Conclusions

The goal of this research was to investigate the structural and physical characteristics of the composite. To identify and distinguish the characteristics of the composite, it was divided into five distinct samples, each with a different fiber loading. The CS sample, which has no fiber reinforcement, serves as the major comparator for all the other samples that have 5–20% SPF loading as a reinforcing agent. Physical and structural tests are carried out in detail to examine the characteristics of the samples in-depth. In terms of densities for each sample, we can conclude that films with 20% fiber loadings are the least dense (1.280 g/cm³) compared to control film (1.528 g/cm³), since sugar palm fiber (*ijuk*) has holes inside the fiber, which led to the films' densities being reduced. The desired outcome in terms of moisture content was not achieved since the SPF-20/CS film did not have the maximum value. Natural fiber is more likely to be hydrophilic, which means it absorbs water. As a result, the films with the greatest fiber loadings should have the highest moisture content. Many elements come into play to develop a pleasing biodegradable composite that can be utilized successfully. The mechanical testing findings demonstrated that gradually increasing the fiber loading from 0% to 5%, increased the tensile strength from 11.33 MPa to 11.78 MPa. Moreover, the study concluded that the sugar palm fiber reinforced cassava starch biopolymer composite could be utilized as a packaging material that is environmentally friendly, but only if its feature of being insoluble in water is improved for future uses.

Highlights

- Sugar palm (*Arenga pinnata* (Wurmb. Merr)) fiber reinforced cassava starch biopolymer composites were developed.
- The addition of SPF into CS film accelerates the biodegradation process of biopolymer composite films.
- The information about the influence of SPF loadings on the physical and mechanical properties of the films could be helpful in the development of biopackaging films.

Acknowledgements

Authors would like to acknowledge Jazan University for providing publication fund and Universiti Putra Malaysia (UPM) for affording research facilities.

Disclosure statement

No potential conflict of interest was reported by the author(s).

Funding

Saeed Abdullah Mousa, College of Engineering, Jazan University, Jazan 706 Saudi Arabia.

Ethical approval

I confirm that all the research meets ethical guidelines and adheres to the legal requirements of the study country.

References

- Abotbina, W., S. M. Sapuan, R. A. Ilyas, M. T. H. Sultan, M. F. M. Alkbir, S. Sulaiman, M. M. Harussani, and E. Bayraktar. 2022. Recent developments in cassava (*Manihot Esculenta*) based biocomposites and their potential industrial applications: A comprehensive review. *Materials* 15 (19):6992. doi:10.3390/ma15196992.
- Abral, H., M. H. Dalimunthe, J. Hartono, R. P. Efendi, M. Asrofi, E. Sugiarti, S. M. Sapuan, J. W. Park, and H. J. Kim. 2018. "Characterization of Tapioca Starch Biopolymer Composites Reinforced with Micro Scale Water Hyacinth Fibers." *Starch* 70 (7–8): 1700287.
- Ayu, R. S., A. Khalina, A. Saffian Harmaen, K. Zaman, T. Isma, R. A. I. Qiuyun Liu, and C. Hao Lee. 2020. Characterization study of empty fruit bunch (EFB) fibers reinforcement in poly(Butylene) succinate (Pbs)/starch/Glycerol composite sheet. *Polymers* 12 (7):1571. doi:10.3390/polym12071571.
- Azlin, M. N. M., R. A. Ilyas, M. Y. M. Zuhri, S. M. Sapuan, M. M. Harussani, S. Sharma, A. H. Nordin, N. M. Nurazzi, and A. N. Afiqah. 2022. 3D printing and shaping polymers, composites, and nanocomposites: A review. *Polymers* 14 (1):180. doi:10.3390/polym14010180.
- Bootklad, M., and K. Kaewtatip. 2013. Biodegradation of thermoplastic starch/eggshell powder composites. *Carbohydrate Polymers* 97 (2):315–20. doi:10.1016/j.carbpol.2013.05.030.
- Chen, S., W. Min, C. Wang, S. Yan, L. Peng, and S. Wang. 2020. Developed Chitosan/Oregano essential oil biocomposite packaging film enhanced by Cellulose Nanofibril. *Polymers* 12 (8):1780. doi:10.3390/polym12081780.
- Chinma, C. E., C. Chukwuma Ariahu, and J. Oneh Abu. 2013. Chemical composition, functional and pasting properties of cassava starch and soy protein concentrate blends. *Journal of Food Science and Technology* 50 (6):1179–85. doi:10.1007/s13197-011-0451-8.
- Dularia, C., A. Sinhmar, R. Thory, A. Kumar Pathera, and V. Nain. 2019. Development of starch nanoparticles based composite films from non-conventional source - water chestnut (*Trapa Bispinosa*). *International Journal of Biological Macromolecules* 136:1161–68. doi:10.1016/j.ijbiomac.2019.06.169.
- Edhirej, A., N. I. Edhirej, S. M. Sapuan, M. Jawaid, M. J. Zahari, and N. Ismarrubie Zahari. 2017. Preparation and characterization of cassava bagasse reinforced thermoplastic cassava starch. *Fibers and Polymers* 18 (1):162–71. doi:10.1007/s12221-017-6251-7.
- Edhirej, A., S. Mohd Sapuan, M. Jawaid, and N. Ismarrubie Zahari. 2017a. Cassava: Its polymer, fiber, composite, and application. *Polymer Composites* 38 (3):555–70. doi:10.1002/pc.23614.
- Edhirej, A., S. Mohd Sapuan, M. Jawaid, and N. Ismarrubie Zahari. 2017b. Effect of various plasticizers and concentration on the physical, thermal, mechanical, and structural properties of cassava-starch-based films. *Starch/staerke* 69 (1–2):1–11. doi:10.1002/star.201500366.
- Edhirej, A., S. M. Sapuan, M. Jawaid, and N. Ismarrubie Zahari. 2017c. Cassava/Sugar palm fiber reinforced cassava starch hybrid composites: Physical, thermal and structural properties. *International Journal of Biological Macromolecules* 101:75–83. doi:10.1016/j.ijbiomac.2017.03.045.
- Farias, J. G. G. D., R. Cordeiro Cavalcante, B. Rodrigues Canabarro, H. Magalhães Viana, S. Scholz, and R. Antoun Simão. 2017. Surface lignin removal on coir fibers by plasma treatment for improved adhesion in thermoplastic starch composites. *Carbohydrate Polymers* 165:429–36. doi:10.1016/j.carbpol.2017.02.042.
- Faruk, O., A. K. Bledzki, H.-P. Fink, and M. Sain. 2012. Biocomposites reinforced with natural fibers: 2000–2010. *Progress in Polymer Science* 37 (11):1552–96. doi:10.1016/j.progpolymsci.2012.04.003.
- Galdeano, M. C., M. V. E. Grossmann, S. Mali, L. A. Bello-Perez, M. A. Garcia, and P. B. Zamudio-Flores. 2009. Effects of production process and plasticizers on stability of films and sheets of oat starch. *Materials Science and Engineering C* 29 (2):492–98. doi:10.1016/j.msec.2008.08.031.
- Gürler, N., S. Paşa, Ö. Erdoğan, and O. Cevik. 2023. Physicochemical properties for food packaging and toxicity behaviors against healthy cells of environmentally friendly biocompatible Starch/Citric Acid/Polyvinyl alcohol biocomposite films. *Starch/staerke* 75 (3–4):1–10. doi:10.1002/star.202100074.
- Hafila, K. Z., R. Jumaidin, R. A. Ilyas, M. Z. Selamat, and F. Asyadi Md Yusof. 2022. Effect of palm wax on the mechanical, thermal, and moisture absorption properties of thermoplastic cassava starch composites. *International Journal of Biological Macromolecules* 194:851–60. doi:10.1016/j.ijbiomac.2021.11.139.
- Han, H. S., and K. Bin Song. 2021. Noni (*Morinda Citrifolia*) fruit polysaccharide films containing blueberry (*Vaccinium Corymbosum*) leaf extract as an antioxidant packaging material. *Food Hydrocolloids* 112 (June 2020). doi: 10.1016/j.foodhyd.2020.106372.
- Haque, M. M., M. Rejaul Haque, M. R. Munshi, S. S. Alam, M. Hasan, M. A. Gafur, F. Rahman, M. Firdaus, and S. Ahmod. 2021. Physico-mechanical properties investigation of sponge-gourd and betel nut reinforced hybrid polyester composites. *Advances in Materials and Processing Technologies* 7 (2):304–16. doi:10.1080/2374068X.2020.1766298.

- Harussani, M. M., S. M. Sapuan, A. Khalina, U. Rashid, and J. Tarique. 2021. Slow pyrolysis of disinfected COVID-19 non-woven polypropylene (PP) waste. *International Symposium on Applied Sciences and Engineering ISASE2021* (May):310–12.
- Harussani, M. M., S. M. Sapuan, U. Rashid, and A. Khalina. 2021. Development and characterization of polypropylene waste from personal protective equipment (PPE)-derived char-filled sugar palm starch biocomposite briquettes. *Polymers* 13 (11):1707. doi:10.3390/polym13111707.
- Harussani, M. M., S. M. Sapuan, U. Rashid, A. Khalina, and R. A. Ilyas. 2022. Pyrolysis of polypropylene plastic waste into Carbonaceous Char: Priority of plastic waste management amidst COVID-19 pandemic. *Science of the Total Environment* 803:149911. doi:10.1016/j.scitotenv.2021.149911.
- Hazrati, K. Z., S. M. Sapuan, M. Y. M. Zuhri, and R. Jumaidin. 2021. Preparation and characterization of starch-based biocomposite films reinforced by *Dioscorea hispida* fibers. *Journal of Materials Research and Technology* 15:1342–55. doi:10.1016/j.jmrt.2021.09.003.
- Ibrahim, M. I. J., S. M. Sapuan, E. S. Zainudin, and M. Y. M. Zuhri. 2019a. Physical, thermal, morphological, and tensile properties of cornstarch-based films as affected by different plasticizers. *International Journal of Food Properties* 22 (1):925–41. doi:10.1080/10942912.2019.1618324.
- Ibrahim, M. I. J., S. M. Sapuan, E. S. Zainudin, and M. Y. M. Zuhri. 2019b. Potential of using multiscale corn husk fiber as reinforcing filler in cornstarch-based biocomposites. *International Journal of Biological Macromolecules* 139:596–604. doi:10.1016/j.ijbiomac.2019.08.015.
- Ilyas, R. A., S. M. Sapuan, M. S. N. Atikah, R. Ibrahim, M. D. Hazrol, S. F. K. Sherwani, T. Jamal, A. Nazrin, and R. Syafiq. 2020. “Natural fibre: A promising source for the production of nanocellulose” 2020 (November): 2–9.
- Ilyas, R. A., S. M. Sapuan, M. R. Ishak, and E. S. Zainudin. 2018. Development and characterization of sugar palm nanocrystalline cellulose reinforced sugar palm starch bionanocomposites. *Carbohydrate Polymers* 202 (May):186–202. doi:10.1016/j.carbpol.2018.09.002.
- Ishak, M. R., S. M. Sapuan, Z. Leman, M. Z. A. Rahman, and U. M. K. Anwar. 2012. Characterization of sugar palm (*Arenga Pinnata*) fibres tensile and thermal properties. *Journal of Thermal Analysis and Calorimetry* 109 (2):981–89. doi:10.1007/s10973-011-1785-1.
- Jaafar, J., J. P. Siregar, A. N. Oumer, M. H. M. Hamdan, C. Tezara, and M. S. Salit. 2018. “Experimental Investigation on Performance of Short Pineapple Leaf Fiber Reinforced Tapioca Biopolymer Composites.” *BioResources* 13 (3): 6341–6355.
- Jaiswal, D., G. L. Devnani, G. Rajeshkumar, M. R. Sanjay, and S. Siengchin. 2022. Review on extraction, characterization, surface treatment and thermal degradation analysis of new cellulosic fibers as sustainable reinforcement in polymer composites. *Current Research in Green and Sustainable Chemistry* 5:100271. doi:10.1016/j.crgsc.2022.100271.
- Jawaid, M., and H. P. S. Abdul Khalil. 2011. Cellulosic/Synthetic fibre reinforced polymer hybrid composites: A review. *Carbohydrate Polymers* 86 (1):1–18. doi:10.1016/j.carbpol.2011.04.043.
- Jouki, M., N. Khazaei, M. Ghasemlou, and M. Hadinezhad. 2013. Effect of glycerol concentration on edible film production from cress seed carbohydrate gum. *Carbohydrate Polymers* 96 (1):39–46. doi:10.1016/j.carbpol.2013.03.077.
- Jumaidin, R., Z. Asyul Sutan Saidi, R. Ahmad Ilyas, M. Nazri Ahmad, M. Khalid Wahid, M. Yuhazri Yaakob, N. Ain Maidin, M. Hidayat Ab Rahman, and M. Hairizal Osman. 2019. Characteristics of cogon grass fibre reinforced thermoplastic cassava starch biocomposite: Water absorption and physical properties. *Journal of Advanced Research in Fluid Mechanics and Thermal Sciences* 62 (1):43–52.
- Jumaidin, R., M. A. A. Khiruddin, Z. A. S. Saidi, M. S. Salit, and R. A. Ilyas. 2020. “Effect of Cogon Grass Fibre on the Thermal, Mechanical and Biodegradation Properties of Thermoplastic Cassava Starch Biocomposite.” *International Journal of Biological Macromolecules* 146:746–755.
- Kaisangsri, N., O. Kerdchoechuen, and N. Laohakunjit. 2012. Biodegradable foam tray from cassava starch blended with natural fiber and chitosan. *Industrial Crops and Products* 37 (1):542–46. doi:10.1016/j.indcrop.2011.07.034.
- Kamaruddin, Z. H., R. Jumaidin, R. Ahmad Ilyas, M. Zulkefli Selamat, R. Hanim Alamjuri, and F. Asyadi Md Yusof. 2022. Influence of alkali treatment on the mechanical, thermal, water absorption, and biodegradation properties of *Cymbopogon citratus* fiber-reinforced, thermoplastic cassava starch–palm wax composites. *Polymers* 14 (14):2769. doi:https://doi.org/10.3390/polym14142769.
- Kuciel, S., and A. Liber-Knec. 2009. Biocomposites on the base of thermoplastic starch filled by Wood and Kenaf Fiber. *Journal of Biobased Materials and Bioenergy* 3 (3):269–74. doi:10.1166/jbmb.2009.1026.
- Ludueña, L., A. Vázquez, and V. Alvarez. 2012. Effect of lignocellulosic Filler type and content on the behavior of polycaprolactone based eco-composites for packaging applications. *Carbohydrate Polymers* 87 (1):411–21. doi:10.1016/j.carbpol.2011.07.064.
- Maran, J. P., V. Sivakumar, K. Thirugnanasambandham, and R. Sridhar. 2014. Degradation behavior of biocomposites based on cassava starch buried under indoor soil conditions. *Carbohydrate Polymers* 101:20–28. doi:10.1016/j.carbpol.2013.08.080.
- Mohammed, A. A. B. A., Z. Hasan, A. A. B. Omran, A. M. Elfaghi, M. A. Khattak, R. A. Ilyas, and S. M. Sapuan. 2023. Effect of various plasticizers in different concentrations on physical, thermal, mechanical, and structural properties of wheat starch-based films. *Polymers* 15 (1):63. doi:10.3390/polym15010063.

- Mohd Nurazzi, N., A. Khalina, S. Mohd Sapuan, and M. Rahmah. 2018. Development of sugar palm Yarn/Glass fibre reinforced unsaturated polyester hybrid composites. *Materials Research Express* 5 (4):045308. doi:10.1088/2053-1591/aabc27.
- Nagarjun, J., J. Kanchana, and G. Rajesh Kumar. 2022. Improvement of mechanical properties of Coir/Epoxy composites through hybridization with sisal and Palmyra palm fibers. *Journal of Natural Fibers* 19 (2):475–84. doi:10.1080/15440478.2020.1745126.
- Norizan, M. N., M. Harussani Moklis, A. Humaira Alias, A. Ilyas Rushdan, M. Nor Faiz Norrrahim, K. Abdan, and N. Abdullah. 2021. Treatments of natural fibre as reinforcement in polymer composites-short review. *Functional Composites & Structures* 3 (2):024002. doi:10.1088/2631-6331/abff36.
- Nurazzi, N. M., F. A. Sabaruddin, M. M. Harussani, S. H. Kamarudin, M. Rayung, M. R. M. Asyraf, H. A. Aisyah. 2021. Mechanical performance and applications of CNTs reinforced polymer composites—A review. *Nanomaterials* 11 (9):2186. doi:10.3390/nano11092186.
- Panichnumsin, P., A. Nopharatana, B. Ahring, and P. Chairprasert. 2010. Production of methane by co-digestion of Cassava Pulp with various concentrations of pig manure. *Biomass and Bioenergy* 34 (8):1117–24. doi:10.1016/j.biombioe.2010.02.018.
- Podshivalov, A., M. Zakharova, E. Glazacheva, and M. Uspenskaya. 2017. Gelatin/Potato starch edible biocomposite films: Correlation between morphology and physical properties. *Carbohydrate Polymers* 157:1162–72. doi:10.1016/j.carbpol.2016.10.079.
- Prachayawarakorn, J., S. Chaiwatyothin, S. Mueangta, and A. Hanchana. 2013. Effect of jute and kapok fibers on properties of thermoplastic cassava starch composites. *Materials & Design* 47 (May):309–15. doi:10.1016/j.matdes.2012.12.012.
- Prachayawarakorn, J., and W. Pattanasin. 2016. Effect of pectin particles and cotton fibers on properties of thermoplastic cassava starch composites. *Journal of Science & Technology* 38 (2):129–36.
- Rajeshkumar, G., S. Arvindh Seshadri, G. L. Devnani, M. R. Sanjay, S. Siengchin, J. P. Maran, N. Abdullah Al-Dhabi. 2021. Environment friendly, renewable and sustainable poly lactic acid (PLA) based natural fiber reinforced composites – a comprehensive review. *Journal of Cleaner Production* 310:127483. doi:10.1016/j.jclepro.2021.127483.
- Roslim, M., Z. L. Muhammad Huzaifah, S. Sapuan, M. Ishak, and R. A. Ilyas. 2018. “Effect of soil burial on water absorption of sugar palm fibre reinforced vinyl ester composites.” In.
- Sahari, J., S. M. Sapuan, Z. N. Ismarrubie, and M. Z. Rahman. 2012. Physical and chemical properties of different morphological parts of sugar palm fibres. *Fibres & Textiles in Eastern Europe* 91 (2):21–24.
- Sahari, J., S. M. Sapuan, Z. N. Ismarrubie, and M. Z. A. Rahman. 2012. Tensile and impact properties of different morphological parts of sugar palm fibre-reinforced unsaturated polyester composites. *Polymers and Polymer Composites* 20 (9):861–66. doi:10.1177/096739111202000913.
- Sahari, J., S. M. Sapuan, E. S. Zainudin, and M. A. Maleque. 2014. Physico-chemical and thermal properties of starch derived from sugar palm tree (*Arenga Pinnata*). *Asian Journal of Chemistry* 26 (4):955–59. doi:10.14233/ajchem.2014.15652.
- Salgado, P. R., V. C. Schmidt, S. E. Molina Ortiz, A. N. Mauri, and J. B. Laurindo. 2008. Biodegradable foams based on cassava starch, sunflower proteins and cellulose fibers obtained by a baking process. *Journal of Food Engineering* 85 (3):435–43. doi:10.1016/j.jfoodeng.2007.08.005.
- Sanyang, M. L., S. M. Sapuan, M. Jawaid, M. R. Ishak, and J. Sahari. 2015. Effect of plasticizer type and concentration on tensile, thermal and barrier properties of biodegradable films based on sugar palm (*Arenga Pinnata*) starch. *Polymers* 7 (6):1106–24. doi:10.3390/polym7061106.
- Sapuan, S. M., and D. Bachtiar. 2012. Mechanical properties of sugar palm fibre reinforced high impact polystyrene composites. *Procedia Chemistry* 4 (May 2014):101–06. doi:10.1016/j.proche.2012.06.015.
- Shakuntala, O., G. Raghavendra, and A. Samir Kumar. 2014. Effect of filler loading on mechanical and tribological properties of wood apple shell reinforced epoxy composite. *Advances in Materials Science and Engineering* 2014:1–9. doi:https://doi.org/10.1155/2014/538651.
- Soykeabkaew, N., P. Supaphol, and R. Rujiravanit. 2004. Preparation and characterization of jute-and flax-reinforced starch-based composite foams. *Carbohydrate Polymers* 58 (1):53–63. doi:10.1016/j.carbpol.2004.06.037.
- Sundum, T., K. Mészáros Szécsényi, and K. Kaewtatip. 2018. Preparation and characterization of thermoplastic starch composites with fly ash modified by planetary ball milling. *Carbohydrate Polymers* 191:198–204. doi:10.1016/j.carbpol.2018.03.009.
- Syafri, E., A. Kasim, H. Abrial, and A. Asben. 2018. Cellulose nanofibers isolation and characterization from ramie using a chemical-ultrasonic treatment. *Journal of Natural Fibers* 0 (00):1–11. doi:10.1080/15440478.2018.1455073.
- Tarique, J., S. Mohd Sapuan, and A. Khalina. 2022. Extraction and characterization of a novel natural lignocellulosic (bagasse and husk) fibers from arrowroot (*Maranta Arundinacea*). *Journal of Natural Fibers* 19 (15):9914–30. doi:10.1080/15440478.2021.1993418.
- Tarique, J., S. M. Sapuan, and A. Khalina. 2021. Effect of glycerol plasticizer loading on the physical, mechanical, thermal, and barrier properties of Arrowroot (*Maranta Arundinacea*) starch biopolymers. *Scientific Reports* 11 (1):13900. doi:10.1038/s41598-021-93094-y.

- Tarique, J., S. M. Sapuan, A. Khalina, R. A. Ilyas, and E. S. Zainudin. 2022c. Thermal, flammability, and antimicrobial properties of arrowroot (*Maranta Arundinacea*) fiber reinforced arrowroot starch biopolymer composites for food packaging applications. *International Journal of Biological Macromolecules* 213 (January):1–10. doi:10.1016/j.ijbio mac.2022.05.104.
- Tarique, J., S. M. Sapuan, A. Khalina, S. F. K. Sherwani, J. Yusuf, and R. A. Ilyas. 2021. Recent developments in sustainable arrowroot (*Maranta Arundinacea* Linn) starch biopolymers, fibres, biopolymer composites and their potential industrial applications: A review. *Journal of Materials Research and Technology* 13 (July):1191–219. doi:10.1016/j.jmrt.2021.05.047.
- Tarique, J., S. M. Sapuan, E. S. Zainudin, A. Khalina, and R. A. Ilyas. 2022a. Degradation behaviour of arrowroot fibre (*Maranta Arundinacea*) reinforced arrowroot starch biocomposite films. *Journal of Research in Nanoscience and Nanotechnology* 5 (1):98–102. doi:10.37934/jrnn.5.1.98102.
- Tarique, J., E. S. Zainudin, S. M. Sapuan, R. A. Ilyas, and A. Khalina. 2022b. Physical, mechanical, and morphological performances of arrowroot (*Maranta Arundinacea*) fiber reinforced arrowroot starch biopolymer composites. *Polymers* 14 (3):388. doi:10.3390/polym14030388.
- Thakur, R., V. Gupta, T. Ghosh, and A. Baran Das. 2022. Effect of anthocyanin-natural deep eutectic solvent (lactic Acid/ Fructose) on mechanical, thermal, barrier, and PH-Sensitive properties of polyvinyl alcohol based edible films. *Food Packaging and Shelf Life* 33 (February):100914. doi:10.1016/j.fpsl.2022.100914.
- Tongdeesoontorn, W., L. J. Mauer, S. Wongruong, P. Sriburi, and P. Rachtanapun. 2012. Mechanical and physical properties of cassava starch-gelatin composite films. *International Journal of Polymeric Materials and Polymeric Biomaterials* 61 (10):778–92. doi:10.1080/00914037.2011.610049.
- Veiga, J. P. S., T. Losada Valle, J. Carlos Feltran, and W. Antonio Bizzo. 2016. Characterization and productivity of cassava waste and its use as an energy source. *Renewable Energy* 93:691–99. doi:10.1016/j.renene.2016.02.078.
- Versino, F., and M. Alejandra García. 2014. Cassava (*Manihot Esculenta*) starch films reinforced with natural fibrous filler. *Industrial Crops and Products* 58:305–14. doi:10.1016/j.indcrop.2014.04.040.
- Walster, R. J., A. R. Rozyanty, A. W. M. Kahar, and L. Musa. 2018. “Study of Cassava Starch Filled with Different Loading of Kenaf Core Fiber.” *Solid State Phenomena* 280:368–373.
- Zhong, Y., and L. Yunfei. 2014. Effects of glycerol and storage relative humidity on the properties of kudzu starch-based edible films. *Starch/staerke* 66 (5–6):524–32. doi:10.1002/star.201300202.